A finite element approach to the immersed boundary method

Daniele Boffi* and Lucia Gastaldi+ and Luca Heltai*

*Dipartimento di Matematica "F. Casorati", Via Ferrata 1, I-27100 Pavia, Italy
+Dipartimento di Matematica, Via Valotti 9, I-25133 Brescia, Italy

Abstract

The immersed boundary method was introduced by Peskin in [31] to study the blood flow in the heart and further applied to many situations where a fluid interacts with an elastic structure. The basic idea is to consider the structure as a part of the fluid where additional forces are applied and additional mass is localized. The forces exerted by the structure on the fluid are taken into account as a source term in the Navier-Stokes equations and are mathematically described as a Dirac delta function lying along the immersed structure. In this paper we first review on various ways of modeling the elastic forces in different physical situations. Then we focus on the discretization of the immersed boundary method by means of finite elements which can handle the Dirac delta function variationally avoiding the introduction of its regularization. Practical computational aspects are described and some preliminary numerical experiment in two dimensions are reported.

Keywords: immersed boundary method, finite element method.

1 Introduction

Fluid-structure interaction systems often involve the resolution of the fluid dynamic equations on a moving (that is, time dependent) domain. Several approaches have been considered in order to deal with such problem. A classical way to overcome the difficulties due to the reconstruction of the mesh at each time step, is the introduction of the arbitrary Lagrangian-Eulerian (ALE) formulation [8, 26, 18, 19, 22, 23], transporting the equations to a fixed arbitrary reference configuration. Although this approach has been used successfully, its accurate implementation is expensive in real applications. In order to be able to solve at low cost fluid structure interaction problems undergoing moderate deformations, aeronautical engineers have developed transpiration techniques, introducing suitable modifications of the interface boundary conditions (see, e.g., [33, 10, 12, 11]).

The fictitious domain method can also be used in order to simulate an incompressible viscous flow around moving rigid bodies; the idea consists in extending the equations to a simple domain where a structured grid can be used and then considering suitable Lagrange multipliers to enforce the boundary conditions along the moving bodies, see [15, 16]. Unfortunately, this method is not able to deal with the interaction between fluid and flexible solids with large deformations.

A completely different approach is due to Peskin who developed the immersed boundary method (IBM) (see [31, 27]) to study flow patterns around heart valves. The immersed boundary method is designed to handle a flexible boundary immersed in a fluid, hence it is particularly suited for biological fluid dynamic problems (see, e.g., [34, 29, 37, 38, 13, 14, 7, 9, 3]. As we have already mentioned, the computation requirement to evolve or adapt the mesh becomes considerably expensive in many fluid-structure interaction systems. In the IBM, the structure is thought as a part of the fluid where additional forces are applied, and where additional mass may be localized. Therefore, instead of separating the system in its two components coupled by interface conditions, as it is conventionally done (see, e.g. [2, 32]), the incompressible Navier-Stokes equations, with a nonuniform mass density and an applied elastic force density, are used in order to describe the coupled motion of the hydroelastic system in a unified way. The advantage of this method is that the fluid domain can have a simple shape, so that structured grids can be used. On the other hand, the immersed boundary is typically not aligned with the grid and it is represented using Lagrangian variables, defined on a curvilinear mesh moving through the domain. Another fundamental assumption of the IBM is that the immersed structure has a fiber-like one dimensional structure, which may have a mass but occupies no volume in the fluid domain (see [27, 34]).

The original numerical approach to the IBM is based on finite differences for the spatial discretization. This employs two independent grids, one for the Eulerian variables in the fluid and the other for the Lagrangian variables associated with the immersed boundary. The main difficulty in the spatial discretization consists in the construction of suitable approximation of the Dirac delta function which is used to take into account the interaction equations, see [27]. The temporal discretization that is currently used by Peskin and his coauthors is a second-order accurate Runge-Kutta method, based on the midpoint rule (see, e.g., [21, 25]).

More recently, the finite element method has been applied to the spatial discretization of the IBM in [4, 5, 35, 36]. In particular, in [35, 36] it has been proposed the EIBM, *extended immersed boundary method* which is based on the idea of considering the submerged elastic solid occupying a finite volume in the fluid domain. This was done by replacing the kinematic and dynamic matching of the fluid-solid interface and the effect of the immersed solid with nodal forces calculated in the context of finite element formulations. The equations in both fluid and solid domains are approximated using finite elements, while the continuity between the fluid and the solid domains are enforced interpolating the velocities and the distribution of forces delta function with the reproducing kernel particle method (RKPM). This enables the construction of dis-

cretized delta function which belongs to $\mathbf{C}^n$ with n chosen according to the required smoothness.

Our approach to the discretization of the IBM is completely based upon the finite element method. Our aim is to deal with the delta function, which is related to the forces exerted by the immersed structure on the fluid and viceversa, in a variational way. So that there is no need to construct a regularization of the delta function, but its effect is taken into account by its action on the test functions.

The outline of the paper is the following. In Sect. 2 we recall the formulation of the IBM and deduce the equivalence with a fluid-structure interaction system in the standard decoupled model. In Sect. 3 we introduce a variational formulation of the IBM which is useful in the spatial finite element discretization. Sect.s 4 and 6 are devoted to the finite element discretization of two models in two and three dimensions respectively. In particular they contain the details on an efficient computational procedure to evaluate the force term along the immersed boundary in the Navier-Stokes equations and several numerical experiments for the two dimensional case are reported in Sect. 5.

2 Formulation of the immersed boundary method

The aim of this section is to review the immersed boundary method and to show how it can model the fluid flow interacting with a flexible or elastic structure. Typically, the immersed material has been modeled as a collections of fibers, see, e.g., [34] for details and [27] for references to many applications. A different approach to the description of an immersed elastic solid can be found in [13, 35, 36].

Let Ω be the two or a three dimensional domain containing the fluid and the flexible or elastic structure. As usual the Navier-Stokes equations describe the dynamics of a viscous incompressible fluid with respect to the Eulerian variables denoted by $\mathbf{x}$:

$$\begin{aligned} &\rho\left(\frac{\partial \mathbf{u}}{\partial t}+\mathbf{u}\cdot\nabla\,\mathbf{u}\right)-\mu\Delta\mathbf{u}+\nabla\, p=\mathbf{F} && \text{in } \Omega\times]0,T[\\ &\nabla\cdot\mathbf{u}=0 && \text{in } \Omega\times]0,T[. \end{aligned} \tag{1}$$

Here ρ and μ denote the density and the viscosity of the fluid. The unknowns $\mathbf{u}(\mathbf{x},t)$ and $p(\mathbf{x},t)$ represent the velocity and the pressure, respectively. On the right hand side of the first equation in (1), $\mathbf{F}$ denotes the density of the body force acting on the fluid. It usually contains a singular vector field, which is zero everywhere, except possibly on the surface representing the immersed structure. We assume that μ is constant, while ρ can be a function of $(\mathbf{x},t)$, since we consider the structure as a part of the fluid carrying an additional mass.

The immersed boundary is considered as an elastic incompressible material filling a two or three dimensional space or laying along an immersed boundary in the form of a simple closed curve or surface. Let $\mathbf{q}$ denote the Lagrangian coordinates in the initial solid domain Ω_0, labeling a material point of it. The position of a point in the current

solid domain at a time t is denoted by $\mathbf{X}(\mathbf{q},t)$, hence this represents the position in Ω of the material point which was labeled by $\mathbf{q}$ at the initial time. Usually the fluid is assumed to have a uniform mass density ρ_0, while the mass density of the immersed structure can be described introducing the *excess* Lagrangian mass density $M(\mathbf{q})$, that is the difference between the mass of the elastic material and the mass of the fluid displaced by it. Then we can express the density of the fluid and the force exerted by the structure on the fluid in terms of $M(\mathbf{q})$, the excess of mass density, and of $\mathbf{f}(\mathbf{q},t)$, the force density that the immersed material applies on the fluid, as follows:

$$\rho(\mathbf{x},t) = \rho_0 + \int_{\Omega_0} M(\mathbf{q})\delta(\mathbf{x}-\mathbf{X}(\mathbf{q},t))\mathrm{d}\mathbf{q}, \qquad \text{in } \Omega\times]0,T[, \tag{2}$$

$$\mathbf{F}(\mathbf{x},t) = \int_{\Omega_0} \mathbf{f}(\mathbf{q},t)\delta(\mathbf{x}-\mathbf{X}(\mathbf{q},t))\mathrm{d}\mathbf{q}, \qquad \text{in } \Omega\times]0,T[, \tag{3}$$

where δ is the Dirac delta function in $\mathbb{R}^3$. The force $\mathbf{F}$ given in (3) is the right hand side of (1) and takes into account the interaction between the fluid and the immersed structure. This is a crucial point in the modeling of different applications, since the expression of $\mathbf{f}$ takes into account the elasticity properties of the structure. In the next subsection we shall review some examples in two and three dimensions which can be found in the literature.

In order to compute the position of the immersed structure another relation which enforces the no slip condition for a viscous fluid has to be considered:

$$\frac{\partial \mathbf{X}}{\partial t} = \mathbf{u}(\mathbf{X}(\mathbf{q},t),t) \qquad \text{in } \Omega_0\times]0,T[. \tag{4}$$

The above equation means that the structure moves at the same velocity as the fluid.

To summarize, the resolution of the immersed boundary method requires to find $\mathbf{u}$, p and $\mathbf{X}$ which satisfy:

$$\rho\left(\frac{\partial \mathbf{u}}{\partial t} + \mathbf{u}\cdot\nabla\,\mathbf{u}\right) - \mu\Delta\mathbf{u} + \nabla\, p = \mathbf{F} \qquad \text{in } \Omega\times]0,T[\tag{5}$$

$$\nabla\cdot\mathbf{u} = 0 \qquad \text{in } \Omega\times]0,T[\tag{6}$$

$$\rho(\mathbf{x},t) = \rho_0 + \int_{\Omega_0} M(\mathbf{q})\delta(\mathbf{x}-\mathbf{X}(\mathbf{q},t))\mathrm{d}\mathbf{q} \quad \text{in } \Omega\times]0,T[\tag{7}$$

$$\mathbf{F}(\mathbf{x},t) = \int_{\Omega_0} \mathbf{f}(\mathbf{q},t)\delta(\mathbf{x}-\mathbf{X}(\mathbf{q},t))\mathrm{d}\mathbf{q} \qquad \text{in } \Omega\times]0,T[\tag{8}$$

$$\frac{\partial \mathbf{X}}{\partial t} = \mathbf{u}(\mathbf{X}(\mathbf{q},t),t) \qquad \text{in } \Omega_0\times]0,T[\tag{9}$$

$$\mathbf{u}(\mathbf{x},t) = 0 \qquad \text{on } \partial\Omega\times]0,T[\tag{10}$$

$$\mathbf{u}(\mathbf{x},0) = \mathbf{u}_0(\mathbf{x}) \qquad \text{in } \Omega \tag{11}$$

$$\mathbf{X}(\mathbf{q},0) = \mathbf{X}_0(\mathbf{q}) \qquad \text{in } \Omega_0. \tag{12}$$

Conditions (10) and (11) represent boundary and initial conditions relative to the Navier-Stokes equation (5)-(6); other boundary conditions could also be used. The

last equation (12) is the initial condition for (9) which drives the motion of the immersed structure. Since $\mathbf{q}$ is the Lagrangian variable associated to a material point in the initial configuration, then $\mathbf{X}_0(\mathbf{q}) = \mathbf{q}$, if we assume that the reference configuration is unstressed.

2.1 Calculation of the elastic forces

The aim of this subsection is to give some ideas on the calculation of the elastic forces exerted by the immersed structure on the fluid. We shall consider two main examples and give a brief description and the references for other approaches and applications. As it can be seen from the variety of applications, the immersed boundary method can produce robust numerical scheme in order to simulate intricate fluid-structure interaction systems.

Example 1 *Massless closed curve immersed in a fluid.*

Let us first consider the simple model problem of a viscous incompressible fluid in a two dimensional square domain Ω containing an immersed massless boundary in the form of a curve (see, e.g., [30, 28]). To be more precise, for all $t \in [0, T]$, let Γ_t be a simple closed elastic curve, the configuration of which is given in a parametric form, $\mathbf{X}(s, t)$, $0 \leq s \leq L$, $\mathbf{X}(0, t) = \mathbf{X}(L, t)$. If the initial configuration is unstressed, the parameter s marks a material point and L is the unstressed length of the boundary. Since we assume that the boundary is massless, then the excess of density mass M in (7) is zero.

The force exerted by the element of boundary ds on the fluid is $\mathbf{f}(s, t)ds$. This force can be computed from the boundary tension $T(s, t)$ and the unit tangent $\boldsymbol{\tau}$ as follows. The tension T is determined by a generalized Hooke's law of the form

$$T = \sigma\left(\left|\frac{\partial \mathbf{X}}{\partial s}\right|; s, t\right). \tag{13}$$

This expression is motivated by the fact that the distance between two points along the curve Γ_t is given by $|\mathrm{d}\mathbf{X}| = |(\partial\mathbf{X}/\partial s)ds|$ and that the distance between the same two points in the reference configuration is $|ds|$. Hence the tension is a function of the ratio of these distances and of s if the material has elastic properties which are not homogeneous in space. Moreover, if the reference configuration is unstressed the strain can be computed as $|\partial\mathbf{X}/\partial s| - 1$.

The direction associated with the tension T is that of the curve itself and it is indicated by the unit tangent

$$\boldsymbol{\tau} = \frac{\partial\mathbf{X}/\partial s}{|\partial\mathbf{X}/\partial s|}. \tag{14}$$

The elastic force acting on a segment between two points $s = a$ and $s = b$ from outside the segment is

$$(T\boldsymbol{\tau})(b, t) - (T\boldsymbol{\tau})(a, t) = \int_a^b \frac{\partial}{\partial s}(T\boldsymbol{\tau})(s, t)ds.$$

Since the curve is massless, this force is transmitted on the fluid occupying the same region as the curve; since a and b are arbitrary, it follows that the local density force applied by the curve to the fluid is given by

$$\mathbf{f} = \frac{\partial}{\partial s}(T\boldsymbol{\tau}). \tag{15}$$

If we assume a stressed initial configuration and T linear with respect to $|\partial\mathbf{X}/\partial s|$, then we obtain from (15)

$$\mathbf{f} = \kappa\frac{\partial^2\mathbf{X}}{\partial s^2}, \tag{16}$$

where κ is the elasticity constant of the material along the immersed boundary.

We observe that problem (5)-(12) can be reduced to a standard formulation in terms of boundary conditions which hold along the immersed elastic interface. In particular in [30] it has been proved that along the immersed curve the following conditions on the jumps of the pressure and the velocity normal derivatives are satisfied:

$$[p] = \frac{\mathbf{f}\cdot\mathbf{n}}{|\partial\mathbf{X}/\partial s|}$$
$$\mu\boldsymbol{\tau}\cdot\left[\frac{\partial\mathbf{u}}{\partial\mathbf{n}}\right] = -\frac{\mathbf{f}\cdot\boldsymbol{\tau}}{|\partial\mathbf{X}/\partial s|},$$

where $[\cdot]$ denotes the jump across the immersed boundary.

Example 2 *Massless elastic membrane immersed in a fluid.*

This case can be seen as a straightforward extension of the previous one. We assume that the fluid domain Ω is a three dimensional cube containing an immersed moving membrane. The membrane Σ_t is represented by $\mathbf{X}(r,s,t)$, where r, s are the parameters of some reference configuration with $0 \le r \le L_r$ and $0 \le s \le L_s$.

The force exerted by the element of boundary $dr\,ds$ on the fluid is $\mathbf{f}(r,s,t)dr\,ds$. Working as above we can calculate the local density force applied by the membrane to the fluid as

$$\mathbf{f} = \frac{\partial}{\partial r}(T_1\boldsymbol{\tau}_1) + \frac{\partial}{\partial s}(T_2\boldsymbol{\tau}_2).$$

Here T_1 and T_2 denote the tension in the r and s directions respectively and can be expressed using a generalized Hooke's law in terms of $|\partial\mathbf{X}/\partial r|$ and $|\partial\mathbf{X}/\partial s|$. The vectors $\boldsymbol{\tau}_1$ and $\boldsymbol{\tau}_2$ are unit vectors on the tangent plane given by

$$\boldsymbol{\tau}_1 = \frac{\partial\mathbf{X}/\partial r}{|\partial\mathbf{X}/\partial r|}, \qquad \boldsymbol{\tau}_2 = \frac{\partial\mathbf{X}/\partial s}{|\partial\mathbf{X}/\partial s|}.$$

If T_1 and T_2 depend linearly on $|\partial\mathbf{X}/\partial r|$ and $|\partial\mathbf{X}/\partial s|$, respectively, then the force can be written as follows:

$$\mathbf{f} = \kappa\Delta_{r,s}\mathbf{X}, \tag{17}$$

where κ is the elasticity constant assuming that the material is homogeneous and isotropic. Here $\Delta_{r,s}$ denotes the Laplacian operator with respect to r and s and $\Delta_{r,s}\mathbf{X}$ is the vector with components $\Delta_{r,s}X_i$ for $i = 1, 2, 3$.

We refer to [20] for the derivation of jump conditions in order to reformulate the governing equations in a standard way.

Example 3 *Elastic fibers immersed in a fluid.*

In many applications, the immersed structure is considered as a system of elastic fibers, with the fiber direction $\boldsymbol{\tau}$ varying smoothly as a function of the position.

Let $(\mathbf{q}, s) \in D$ be material curvilinear coordinates describing the initial configuration D, chosen in such a manner that $\mathbf{q} = (q_1, q_2)$ is constant along each fiber. Then the elastic potential energy of the material can be expressed as a function of the configuration $\mathbf{X}$ at a time t, in the form:

$$E(\mathbf{X}) = \int_D \mathcal{T}\left(\left|\frac{\partial \mathbf{X}}{\partial x}\right|\right) \mathrm{d}\mathbf{q}\, ds,$$

assuming that it depends only on the strain in the fiber direction.

Using the principle of virtual work, the force density $-\mathbf{F}$ is the Fréchet derivative of E that is:

$$\mathbf{F} = -\frac{\partial E}{\partial \mathbf{X}},$$

which, after some calculation using also integration by parts with respect to s, yields:

$$\mathbf{F} = \frac{\partial}{\partial s}\left(\mathcal{T}'\left(\left|\frac{\partial \mathbf{X}}{\partial x}\right|\right) \frac{\partial \mathbf{X}/\partial s}{|\partial \mathbf{X}/\partial s|}\right),$$

where $\mathcal{T}'$ is the derivative of $\mathcal{T}$ and represents the tension in the direction of the fibers (see [27] for the details).

This general framework was used, for example, to model the blood flow in the heart [28, 25], the fluid flow in collapsible elastic tubes [34], a flapping flexible filament in a flowing soap film [37, 38].

Example 4 *Elastic shells immersed in a fluid.*

In [13] an elastic shell immersed in a viscous incompressible fluid is described and the resulting numerical method has been used in [14] to construct a comprehensive three dimensional computational model of the macro-mechanics of the cochlea which incorporates the intricate curved cochlear anatomy. The deformation of the shell is described assuming the Kirchhoff-Love hypothesis. This means that the shell is viewed as a material composed of rigid fibers which remain perpendicular to the middle surface and cannot be stretched during the deformation, so that its deformation is completely determined by the deformation of the middle surface.

Example 5 *Flexible solid occupying a finite volume within the fluid domain.*

A possible drawback of the IBM is the assumptions of the fiber-like one dimensional structure, which may carry mass, but occupies no volume in the fluid. In [35, 36] an incompressible three dimensional deformable structure occupying the region Ω^s is assumed to be immersed in an incompressible fluid domain Ω^f, so that the following relations hold true:

$$\Omega^f \cup \Omega^s = \Omega, \qquad \Omega^f \cap \Omega^s = \emptyset. \tag{18}$$

As usual, if $\mathbf{q} \in \Omega_0^s$ denotes a material point in the initial configuration, then $\mathbf{X}(\mathbf{q}, t)$ represents the position of $\mathbf{q}$ in the current configuration $\Omega^s(t)$. The governing equations of motion are written in a unified way for a continuum containing both fluid and solid, and the interaction between the two components is taken into account as usual by a Dirac delta function. The density force $\mathbf{f}$ in (8) is obtained in a different way from the one presented in the above examples (see [35, 36] for details of the derivation).

Assume that ρ^f and ρ^s denote the fluid density and the solid density, respectively. Then we solve (5)-(6) in the whole domain Ω with $\rho = \rho^f$ and the force $\mathbf{F}$ on the right hand side can be written as follows

$$\begin{aligned} &\mathbf{F}(\mathbf{x}, t) = \int_{\Omega^s(t)} \mathbf{f}(\mathbf{X}(t), t)\delta(\mathbf{x} - \mathbf{X}(t))\mathrm{d}\mathbf{X}, \\ &f_i = -(\rho^s - \rho^f)\frac{\mathrm{d}v_i^s}{\mathrm{d}t} + \sum_{j=1}^{3}(\sigma_{ij,j}^s - \sigma_{ij,j}^f) + (\rho^s - \rho^f)g_i \quad \text{in } \Omega^s(t),\ i = 1, 2, 3, \end{aligned} \tag{19}$$

where g_i represents the gravitational external force and v_i^s the components of the velocity of the solid.

At the end, the Cauchy stress σ_{ij}^s, can be modeled in different ways depending on the material. For example, in [35, 36], the three dimensional almost incompressible hyperelastic material model with the Mooney-Rivlin material description was introduced.

3 Variational formulation of the immersed boundary method

The spatial discretization of IBM has been originally done by means of finite differences. This requires the construction of two independent grids, one for the Eulerian variables and the other for the Lagrangian variables. The only restriction, which is imposed in order to avoid leaks, is that the Lagrangian grid is sufficiently fine in order that the distance between the values of $\mathbf{X}$ at two adjacent points of the Lagrangian grid is less than the Eulerian meshsize h. The main issue is the computation of the force in (8), due to the presence of the Dirac delta function. This has been realized by the construction of a suitable approximation function δ_h, which is nonsingular for each h and approaches δ as $h \to 0$ (we refer to [27] for a detailed description of such construction).

More recently, in [4, 5, 35, 36] a finite element approach to the spatial discretization of the IBM has been proposed. In [35, 36] the finite element scheme is based on a Petrov-Galerkin weak form of the Navier-Stokes equations and a variational formulation of the momentum equation, which governs the deformation of the solid (see the second equation in (19)). The coupling between the fluid and the structure is based on the *reproducing kernel particle method* (RKPM) introduced in [24].

Our spatial discretization is based on the use of standard finite elements in the approximation of the Navier-Stokes equation and on the discretization of the immersed boundary by continuous piecewise linear elements. Our approach is different from that of [35, 36], since we deal with the force term involving the Dirac delta function in a variational way, so that there is no need of approximating the delta function. For simplicity, our presentation refers to Examples 1 and 2, hence in the rest of the paper we shall assume a constant density ρ.

In order to apply a finite element method, we need to introduce a variational formulation of the Navier-Stokes equations. To this aim, we specify a precise definition of the force (8).

In order to work with Examples 1 and 2 in a unified way, let B_t denote the immersed boundary, that is the one dimensional curve Γ_t in the case of Example 1 or the membrane Σ_t in Example 2. Then let $\mathbf{X}(\mathbf{s}, t)$ denote a material point on B_t, where the variable $\mathbf{s}$ gives the parametric representation and varies in a domain D (D is an interval in the case of Example 1 or a rectangle in Example 2). We observe that, in equation (8), the boundary force $\mathbf{F}$ is multiplied by a two or three dimensional Dirac function, over a domain of dimension one or two, respectively, so that the resulting force density $\mathbf{F}$ is a one dimensional Dirac function along B_t and the following Lemma holds true.

Lemma 1 *Assume that, for all $t \in [0, T]$, the immersed boundary B_t is Lipschitz continuous. Then for all $t \in]0, T[$, the force density $\mathbf{F}(t)$, defined formally in (8), is a distribution function belonging to $H^{-1}(\Omega)^d$ ($d = 2, 3$) defined as follows: for all $\mathbf{v} \in H_0^1(\Omega)^d$*

$$ {}_{H^{-1}}\!<\mathbf{F}(t), \mathbf{v}>_{H_0^1} = \int_D \mathbf{f}(\mathbf{s}, t) \cdot \mathbf{v}(\mathbf{X}(\mathbf{s}, t))\, \mathrm{d}\mathbf{s} \quad \forall t \in]0, T[\,. \tag{20} $$

The proof can be obtained extending the one given in [4].

In view of the finite element discretization of the problem, we introduce a variational formulation of equations (5)-(6); hence we have to solve the following problem.

Problem 1 *Given $\mathbf{f} \in L^2(D \times]0, T[)$, $\mathbf{u}_0 \in H_0^1(\Omega)^d$ and $\mathbf{X}_0 : D \to \Omega$, for all*

$t \in]0,T[$, *find* $(\mathbf{u}(t), p(t)) \in H_0^1(\Omega)^d \times L_0^2(\Omega)$ *and* $\mathbf{X} : D \times]0,T[\to \Omega$, *such that*

$$\rho\left(\frac{d}{dt}(\mathbf{u}(t),\mathbf{v}) + (\mathbf{u}\cdot\boldsymbol{\nabla}\,\mathbf{u},\mathbf{v})\right) + \mu(\boldsymbol{\nabla}\,\mathbf{u}(t),\boldsymbol{\nabla}\,\mathbf{v})$$

$$- (\nabla\cdot\mathbf{v}, p(t)) =< \mathbf{F}(t),\mathbf{v} > \qquad \forall \mathbf{v} \in H_0^1(\Omega)^d \qquad (21)$$

$$(\nabla\cdot\mathbf{u}(t), q) = 0 \qquad \forall q \in L_0^2(\Omega) \qquad (22)$$

$$< \mathbf{F}(t),\mathbf{v} >= \int_D \mathbf{f}(\mathbf{s},t)\mathbf{v}(\mathbf{X}(\mathbf{s},t))\,\mathrm{d}\mathbf{s} \qquad \forall \mathbf{v} \in H_0^1(\Omega)^d \qquad (23)$$

$$\frac{\partial \mathbf{X}}{\partial t}(\mathbf{s},t) = \mathbf{u}(\mathbf{X}(\mathbf{s},t),t) \qquad \forall \mathbf{s} \in D \qquad (24)$$

$$\mathbf{u}(\mathbf{x},0) = \mathbf{u}_0(\mathbf{x}) \qquad \forall \mathbf{x} \in \Omega \qquad (25)$$

$$\mathbf{X}(\mathbf{s},0) = \mathbf{X}_0(\mathbf{s}) \qquad \forall \mathbf{s} \in D. \qquad (26)$$

In (21) and (22), $(\cdot,\cdot)$ stands for the usual scalar product in $L^2(\Omega)$, while $< \cdot,\cdot >$ denotes the duality pairing between $H^{-1}(\Omega)^d$ and $H_0^1(\Omega)^d$. We recall that $L_0^2(\Omega)$ is the subset of $L^2(\Omega)$ containing the elements with zero mean value.

We observe that a further condition on $\mathbf{X}$ should be added, so that for all $\mathbf{s} \in D$ and $t \in [0,T]$, we have $\mathbf{X}(\mathbf{s},t) \in \Omega$. However, since we enforce an homogeneous Dirichlet boundary condition on $\mathbf{u}$, equation (24) implies that if $\mathbf{X}$ reaches the boundary of Ω then it remains on $\partial\Omega$ for all the successive times.

To model the force density $\mathbf{f}$, we make use of (16) in the two dimensional case and of (17) in the three dimensional one, which can be written in an unified way as

$$\mathbf{f}(\mathbf{s},t) = \kappa\Delta_{\mathbf{s}}\mathbf{X}(\mathbf{s},t) \qquad (27)$$

where $\Delta_{\mathbf{s}}\mathbf{X}$, denotes the vector of the second derivative with respect to s (respectively, the Laplacian operator with respect to the variables s_1 and s_2) of the components of $\mathbf{X}$ (see (16) and (17)). The following stability estimate holds true for the solution of Problem 1.

Lemma 2 *For* $t \in]0,T[$, *let* $\mathbf{u}(t) \in H_0^1(\Omega)^d$, $p(t) \in L_0^2(\Omega)$ *and* $\mathbf{X}(t) \in (H^1(D))^d$ *be a solution of Problem 1, then it holds:*

$$\frac{\rho}{2}\frac{d}{dt}||\mathbf{u}(t)||_0^2 + \mu||\,\nabla\,\mathbf{u}(t)||_0^2 + \frac{\kappa}{2}\frac{d}{dt}\|\nabla_{\mathbf{s}}\mathbf{X}(t)\|_0^2 = 0, \qquad (28)$$

where $\nabla_{\mathbf{s}}\mathbf{X}$ *denotes the array of the first derivatives of* $\mathbf{X}$ *and* $\|\cdot\|_0$ *stands for the norm in* $L^2(\Omega)$.

Proof. Take $\mathbf{v} = \mathbf{u}$ in (21), use (24), and integrate by parts, recalling also (22). The desired bound then follows. □

The last term on the left hand side of (28) shows that the elastic energy of the immersed boundary is conserved during the motion.

The next two sections are devoted to the introduction of the spatial finite element discretization for a two and a three dimensional problem, respectively; in particular we shall describe in detail how to practically compute (23) using (16) or (17).

4 Finite element discretization of a two dimensional problem

Let us consider the two dimensional situation described in Example 1. The fluid domain Ω is a square region, containing an immersed massless elastic boundary with the form of a simple closed curve Γ_t. Using the notation of the previous section, $D = [0, L]$ is the parametric interval and the points on the curve are represented in parametric form by $\mathbf{X}(s,t)$, $0 \leq s \leq L$. Since the curve is closed we enforce that $\mathbf{X}(0,t) = \mathbf{X}(L,t)$ for $t \in [0,T]$. Taking into account (16), Problem 1 reads:

Problem 2 *Given* $\mathbf{f} \in L^2(]0,L[\times]0,T[)$, $\mathbf{u}_0 \in H_0^1(\Omega)^2$ *and* $\mathbf{X} : [0,L] \to \Omega$, *for all* $t \in]0,T[$, *find* $(\mathbf{u}(t), p(t)) \in H_0^1(\Omega)^2 \times L_0^2(\Omega)$ *and* $\mathbf{X} : [0,L] \times]0,T[\to \Omega$, *such that*

$$\rho\left(\frac{d}{dt}(\mathbf{u}(t),\mathbf{v}) + (\mathbf{u}\cdot\boldsymbol{\nabla}\,\mathbf{u},\mathbf{v})\right) + \mu(\boldsymbol{\nabla}\,\mathbf{u}(t),\boldsymbol{\nabla}\,\mathbf{v})$$
$$-(\nabla\cdot\mathbf{v}, p(t)) =< \mathbf{F}(t),\mathbf{v} > \qquad \forall \mathbf{v} \in H_0^1(\Omega)^2 \qquad (29)$$
$$(\nabla\cdot\mathbf{u}(t), q) = 0 \qquad \forall q \in L_0^2(\Omega) \qquad (30)$$
$$< \mathbf{F}(t),\mathbf{v} >= \int_0^L \kappa \frac{\partial^2 \mathbf{X}(s,t)}{\partial s^2}\mathbf{v}(\mathbf{X}(s,t))\,ds \qquad \forall \mathbf{v} \in H_0^1(\Omega)^2 \qquad (31)$$
$$\frac{\partial \mathbf{X}}{\partial t}(s,t) = \mathbf{u}(\mathbf{X}(s,t),t) \qquad \forall s \in [0,L] \qquad (32)$$
$$\mathbf{u}(\mathbf{x},0) = \mathbf{u}_0(\mathbf{x}) \qquad \forall \mathbf{x} \in \Omega \qquad (33)$$
$$\mathbf{X}(s,0) = \mathbf{X}_0(s) \qquad \forall \mathbf{s} \in [0,L] \qquad (34)$$
$$\mathbf{X}(0,t) = \mathbf{X}(L,t) \qquad \forall t \in [0,T]. \qquad (35)$$

Let us introduce the finite element spaces which will be used in the spatial discretization. Let $\mathcal{T}_h$ be a subdivision of Ω into triangles or rectangles. We denote by h_x the biggest diameter of the elements of $\mathcal{T}_h$. We then consider two finite dimensional subspaces $\mathbf{V}_h \subseteq H_0^1(\Omega)^2$ and $Q_h \subseteq L_0^2(\Omega)$. It is well known that the pair of spaces $\mathbf{V}_h$ and Q_h need to satisfy the inf-sup condition in order to have existence, uniqueness and stability of the discrete solution of the Navier-Stokes problem (29)-(30) (see [17, 6]).

Next, let s_i, $i = 0, \cdots, m$ with $s_0 = 0$ and $s_m = L$, be $m+1$ distinct points of the interval $[0,L]$. We set $h_s = \max_{0\leq i\leq m} |s_i - s_{i-1}|$. Let $\mathbf{S}_h$ be the finite element space of piecewise linear vectors defined on $[0,L]$ as follows

$$\mathbf{S}_h = \{\mathbf{Y} \in C^0([0,L];\Omega) : \ \mathbf{Y}|_{[s_{i-1},s_i]} \in \mathcal{P}^1([s_{i-1},s_i])^2,\ i = 1,\cdots,m, \ \mathbf{Y}(s_0) = \mathbf{Y}(s_m)\} \qquad (36)$$

where $\mathcal{P}^1(I)$ stands for the space of affine polynomials on the interval I. For an element $\mathbf{Y} \in \mathbf{S}_h$ we shall use also the following notation $\mathbf{Y}_i = \mathbf{Y}(s_i)$ for $i = 0, \cdots, m$.

The first step, in order to introduce the discrete counterpart of Problem 2, is the computation of (31) for all $\mathbf{X}_h \in \mathbf{S}_h$ and for all $\mathbf{v} \in \mathbf{V}_h$. We integrate by parts the

integral on the right hand side of (31) taking into account that $\mathbf{X}_{h\,0} = \mathbf{X}_{h\,m}$ and that $\mathbf{v}$ is continuous, then we obtain:

$$< \mathbf{F}_h(t), \mathbf{v} >= -\kappa \int_0^L \frac{\partial \mathbf{X}_h(s,t)}{\partial s} \frac{\partial \mathbf{v}(\mathbf{X}_h(s,t))}{\partial s}\, ds. \tag{37}$$

We write the last integral as a sum over the subintervals $[s_{i-1}, s_i]$, use the fact that $\mathbf{X}_h$ is linear, so that its derivative is constant, and arrive at:

$$\begin{aligned} < \mathbf{F}_h(t), \mathbf{v} > &= -\sum_{i=1}^{m} \kappa \frac{\partial \mathbf{X}_{h\,i}}{\partial s}(t) \int_{s_{i-1}}^{s_i} \frac{\partial \mathbf{v}(\mathbf{X}_h(s,t))}{\partial s}\, ds \\ &= -\sum_{i=1}^{m} \kappa \frac{\partial \mathbf{X}_{h\,i}}{\partial s}(t) \left(\mathbf{v}(\mathbf{X}_{h\,i}(t)) - \mathbf{v}(\mathbf{X}_{h\,i-1}(t))\right), \end{aligned} \tag{38}$$

where $\partial \mathbf{X}_{h\,i}(t)/\partial s$ denotes the derivative of $\mathbf{X}_h(t)$ on $]s_{i-1}, s_i[$.

Reordering the terms in the sum, we get:

$$\begin{aligned} < \mathbf{F}_h(t), \mathbf{v} > &= -\sum_{i=1}^{m} \kappa \frac{\partial \mathbf{X}_{h\,i}}{\partial s}(t) \mathbf{v}(\mathbf{X}_{h\,i}(t)) + \sum_{i=0}^{m-1} \kappa \frac{\partial \mathbf{X}_{h\,i+1}}{\partial s}(t) \mathbf{v}(\mathbf{X}_{h\,i}(t)) \\ &= \sum_{i=0}^{m-1} \kappa \left(\frac{\partial \mathbf{X}_{h\,i+1}}{\partial s}(t) - \frac{\partial \mathbf{X}_{h\,i}}{\partial s}(t) \right) \mathbf{v}(\mathbf{X}_{h\,i}(t)). \end{aligned} \tag{39}$$

Notice that the right hand side of (39) is meaningful, since $\mathbf{v}$ is continuous as it is required for the elements in $\mathbf{V}_h$.

We also observe that it is possible to derive (39) in a different way based on physical interpretation. We can think of the discrete massless elastic boundary as being made of a series of springs joining each two consecutive points $\mathbf{X}_{h\,i}$ and $\mathbf{X}_{h\,i+1}$. Assuming massless springs with zero length at rest and elastic constant γ_i, the force exerted on each of the two points of the segment is proportional to the displacement from the rest position, given by Δx_i, and follows the well known equation for ideal springs:

$$\varphi_i = -\gamma_i \Delta x_i. \tag{40}$$

We note that the elastic constant γ_i in (40) is spring dependent, meaning that in a realistic model of a spring it depends on elastic properties of the material, on the mass of the spring, on its density and on its geometry.

In our case the elongations of the two segments to which the i-th point belongs, are given by $(\mathbf{X}_{h\,i\pm1}(t) - \mathbf{X}_{h\,i}t))$ and they are responsible for pulling the two end points $\mathbf{X}_{h\,i\pm1}(t)$ towards $\mathbf{X}_{h\,i}(t)$. On the other hand, each of the two end points pulls $\mathbf{X}_{h\,i}(t)$ with a force which has the same intensity and the opposite direction, and the resultant is given by:

$$\begin{aligned} \varphi_{h\,i}(\mathbf{X}_{h\,i}(t), t) =& \gamma_i \big(\mathbf{X}_{h\,i+1}(t) - \mathbf{X}_{h\,i}(t)\big) + \gamma_{i-1} \big(\mathbf{X}_h(s_{i-1}, t) - \mathbf{X}_h(s_i, t)\big) \\ =& \gamma_i \frac{\partial \mathbf{X}_{h\,i+1}}{\partial s}(t)(s_{i+1} - s_i) - \gamma_{i-1} \frac{\partial \mathbf{X}_{h\,i}}{\partial s}(t)(s_i - s_{i-1}). \end{aligned} \tag{41}$$

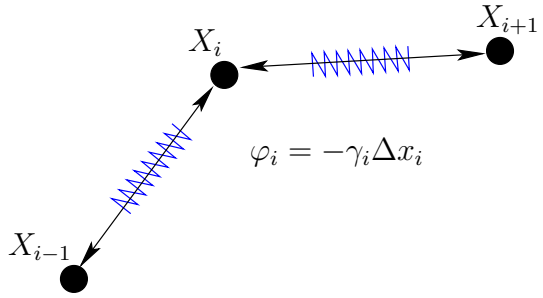

Figure 1: "Spring" interpretation of the boundary

Figure 1 illustrates this interpretation. If we assume the spring constants to be

$$\gamma_i = \kappa \frac{1}{s_{i+1} - s_i}, \tag{42}$$

we obtain an expression of the force equivalent to that presented in (39). Equation (42) shows a possible interpretation we can give to the parametrization. A different parametrization speed changes the elastic properties of the boundary.

As already stated these properties are mass and geometry dependent, but in our model the immersed boundary is thought to be both massless and volumeless. Therefore to reflect the physical meaning of the boundary mass and of its geometry without taking into account their effect on the fluid, the mass and geometry dependencies are incorporated in the elastic constants γ_i by making them dependent on the parametrization, as stated in equation (42). In Section 5.3 we illustrate these dependencies with numerical experiments.

The spatial finite element discretization of Problem 2 reads:

Problem 3 *Given* $\mathbf{f} \in L^2(]0, L[\times]0, T[)$, $\mathbf{u}_{0h} \in \mathbf{V}_h$ *and* $\mathbf{X}_{h\,0} \in \mathbf{S}_h$, *for all* $t \in]0, T[$, *find* $(\mathbf{u}_h(t), p_h(t)) \in \mathbf{V}_h \times Q_h$ *and* $\mathbf{X}_h(t) \in \mathbf{S}_h$, *such that*

$$\rho \left(\frac{d}{dt}(\mathbf{u}_h(t), \mathbf{v}) + (\mathbf{u}_h \cdot \boldsymbol{\nabla}\, \mathbf{u}_h, \mathbf{v}) \right) + \mu(\boldsymbol{\nabla}\, \mathbf{u}_h(t), \boldsymbol{\nabla}\, \mathbf{v})$$
$$- (\nabla \cdot \mathbf{v}, p_h(t)) = < \mathbf{F}_h(t), \mathbf{v} > \qquad \forall \mathbf{v} \in \mathbf{V}_h \tag{43}$$
$$(\nabla \cdot \mathbf{u}_h(t), q) = 0 \qquad \forall q \in Q_h \tag{44}$$
$$< \mathbf{F}_h(t), \mathbf{v} > = \sum_{i=0}^{m-1} \kappa \left(\frac{\partial \mathbf{X}_{h\,i+1}}{\partial s}(t) - \frac{\partial \mathbf{X}_{h\,i}}{\partial s}(t) \right) \mathbf{v}(\mathbf{X}_{h\,i}(t)) \quad \forall \mathbf{v} \in \mathbf{V}_h \tag{45}$$
$$\frac{\partial \mathbf{X}_{h\,i}}{\partial t}(t) = \mathbf{u}_h(\mathbf{X}_{h\,i}(t), t) \qquad \forall i = 0, 1, \cdots, m \tag{46}$$
$$\mathbf{u}_h(\mathbf{x}, 0) = \mathbf{u}_{0h}(\mathbf{x}) \qquad \forall \mathbf{x} \in \Omega \tag{47}$$
$$\mathbf{X}_{h\,i}(0) = \mathbf{X}_0(s_i) \qquad \forall i = 1, \cdots, m. \tag{48}$$

The following discrete counterpart of the stability estimate (28) holds true:

Lemma 3 *For $t \in]0,T[$, let $\mathbf{u}_h(t) \in \mathbf{V}_h$, $p_h(t) \in Q_h$ and $\mathbf{X}_h(t) \in \mathbf{S}_h$ be a solution of Problem 3, then it holds:*

$$\frac{\rho}{2}\frac{d}{dt}\|\mathbf{u}_h(t)\|_0^2 + \mu\| \nabla \mathbf{u}(t)\|_0^2 + \frac{\kappa}{2}\frac{d}{dt}\left\|\frac{\partial \mathbf{X}_h(t)}{\partial s}\right\|_0^2 = 0. \tag{49}$$

Proof. Following the same line as in the proof of the continuous case, let us take $\mathbf{v} = \mathbf{u}_h(t)$ in (43), use (44) and integrate by parts the nonlinear advective term, then we obtain:

$$\frac{\rho}{2}\frac{d}{dt}\|\mathbf{u}_h(t)\|_0^2 + \mu\| \nabla \mathbf{u}_h(t)\|_0^2 = \sum_{i=0}^{m-1} \kappa \left(\frac{\partial \mathbf{X}_{h\,i+1}}{\partial s}(t) - \frac{\partial \mathbf{X}_{h\,i}}{\partial s}(t)\right) \mathbf{u}_h(\mathbf{X}_{h\,i}(t),t). \tag{50}$$

Using (46) and the fact that $\mathbf{X}_h$ is piecewise linear, we can deal with the sum in the right hand side of (50) as follows

$$\begin{aligned}
&\sum_{i=0}^{m-1} \kappa \left(\frac{\partial \mathbf{X}_{h\,i+1}}{\partial s}(t) - \frac{\partial \mathbf{X}_{h\,i}}{\partial s}(t)\right) \mathbf{u}_h(\mathbf{X}_{h\,i}(t),t) \\
&\quad = \sum_{i=0}^{m-1} \kappa \left(\frac{\partial \mathbf{X}_{h\,i+1}}{\partial s}(t) - \frac{\partial \mathbf{X}_{h\,i}}{\partial s}(t)\right) \frac{\partial \mathbf{X}_{h\,i}(t)}{\partial t} \\
&\quad = \kappa \sum_{i=0}^{m-1} \left(\frac{\mathbf{X}_{h\,i+1}(t) - \mathbf{X}_{h\,i}(t)}{s_{i+1}-s_i} - \frac{\mathbf{X}_{h\,i}(t) - \mathbf{X}_{h\,i-1}(t)}{s_i - s_{i-1}}\right) \frac{\partial \mathbf{X}_{h\,i}(t)}{\partial t} \\
&\quad = -\kappa \sum_{i=0}^{m-1} \frac{\mathbf{X}_{h\,i+1}(t) - \mathbf{X}_{h\,i}(t)}{s_{i+1}-s_i} \frac{\partial}{\partial t}(\mathbf{X}_{h\,i+1}(t) - \mathbf{X}_{h\,i}(t)) \\
&\quad = -\frac{\kappa}{2} \sum_{i=0}^{m-1} \frac{1}{s_{i+1}-s_i} \frac{\partial}{\partial t}(\mathbf{X}_{h\,i+1}(t) - \mathbf{X}_{h\,i}(t))^2 \\
&\quad = -\frac{\kappa}{2} \sum_{i=0}^{m-1} \frac{d}{dt} \int_{s_i}^{s_{i+1}} \left(\frac{\partial \mathbf{X}(s,t)}{\partial s}\right)^2 ds = -\frac{\kappa}{2}\frac{d}{dt}\left\|\frac{\partial \mathbf{X}_h(t)}{\partial s}\right\|_0^2.
\end{aligned}$$

The desired estimate is then obtained inserting the last equality in (50). □

Notice that the elasticity energy of the immersed boundary is conserved also in the finite element discretization of Problem 2.

The time discretization is based on the backward Euler method. Let Δt denote the time step and let us indicate by the superscript n an unknown function at time $t_n = n\Delta t$. The number of time steps needed to reach the final time T is N. In Problem 3, the Navier-Stokes equations (43)-(44) are strongly coupled through the source term (45) with the system of ordinary differential equations given by (46). Therefore, in order to avoid the resolution of a fully nonlinear system of equations at each time step, we adopt a natural modification of the backward Euler method. Then, our scheme

consists of two steps: given the approximation $\mathbf{X}_h^n$ of $\mathbf{X}$ at time $n\Delta t$, we construct $\mathbf{F}_h^{n+1}$ and find the solution $(\mathbf{u}_h^{n+1}, p_h^{n+1})$ to the Navier-Stokes equations; then we move the immersed boundary, getting $\mathbf{X}_h^{n+1}$. In the preliminary numerical experiments, which we present at the end of this section, we have considered a linearization of the Navier-Stokes equations, so that the time advancing scheme develops into the following steps.

Given $\mathbf{f} \in L^2(]0, L[\times]0, T[)$, $\mathbf{u}_{0h} \in \mathbf{V}_h$ and $\mathbf{X}_{0h} \in \mathbf{S}_h$, set $\mathbf{u}_h^0 = \mathbf{u}_{0h}$ and $\mathbf{X}_h^0 = \mathbf{X}_{0h}$, then for $n = 0, 1, \cdots, N-1$

Step 1. compute the source term

$$< \mathbf{F}_h^{n+1}, \mathbf{v} >= \sum_{i=0}^{m-1} \kappa \left(\frac{\partial \mathbf{X}_{h\,i+1}^n}{\partial s} - \frac{\partial \mathbf{X}_{h\,i}^n}{\partial s} \right) \mathbf{v}(\mathbf{X}_{h\,i}^n) \qquad \forall \mathbf{v} \in \mathbf{V}_h;$$

Step 2. find $(\mathbf{u}_h^{n+1}, p_h^{n+1}) \in \mathbf{V}_h \times Q_h$, such that

$$\begin{aligned} \rho(\frac{\mathbf{u}_h^{n+1} - \mathbf{u}_h^n}{\Delta t}, \mathbf{v}) + \mu(\boldsymbol{\nabla}\, \mathbf{u}_h^{n+1}, \boldsymbol{\nabla}\, \mathbf{v}) - (\nabla \cdot \mathbf{v}, p_h^{n+1}) & \\ =< \mathbf{F}_h^{n+1}, \mathbf{v} > \quad & \forall \mathbf{v} \in \mathbf{V}_h \\ (\nabla \cdot \mathbf{u}_h^{n+1}, q) = 0 \quad & \forall q \in Q_h \end{aligned}$$

Step 3. find $\mathbf{X}_h^{n+1} \in \mathbf{S}_h$, such that

$$\frac{\mathbf{X}_{h\,i}^{n+1} - \mathbf{X}_{h\,i}^n}{\Delta t} = \mathbf{u}_h^{n+1}(\mathbf{X}_{h\,i}^n) \quad \forall i = 1, \cdots, m.$$

5 Numerical results for the two dimensional formulation

If not stated otherwise, the following examples have been computed with these parameters: the time step is fixed and it is equal to $\Delta t = 0.01$, the domain refinement is always 32 by 32 subsquares per unit square. For the discretization of the linearized Navier-Stokes equations (see Step 2.) we use the well known Q2/P1 element, which is stable.

The examples we present are thought as an overview on the potentiality of this method, and are not intended to reproduce physical problems, therefore all the physical constants have been set to 1 (this is true for ρ, μ and κ).

The expression of the tension (13) has been set to

$$T = \left| \frac{\partial \mathbf{X}}{\partial s} \right|, \tag{51}$$

which corresponds to a model for zero-length, zero-mass ideal elastic material with elastic properties proportional to the speed of parametrization. In Example 5.1 and 5.2

m	16	32	64	128	256	512	1024
$N = 4$	36.4679	35.9438	37.1656	37.9881	38.4128	38.6349	38.7531
$N = 8$	15.9512	14.0895	13.0572	12.8094	12.8091	12.8430	12.8670
$N = 16$	20.1816	9.0145	7.2548	7.0113	7.1047	7.1913	7.2461
$N = 32$	45.2925	9.7634	2.7878	2.3081	2.3033	2.3245	2.3508

Table 1: Percentage of area loss

we show the general behavior of our model, both with and without a superimposed source term. Example 5.3 shows the behavior of the model in presence of a non uniform parametrization of the immersed boundary, highlighting the physical meaning of equation (51) which is also evident in Example 5.4, while in Sections 5.5 and 5.6 we study the interactions between an immersed boundary with the domain boundary $\partial\Omega$ and that between two immersed boundaries, respectively.

The program used to compute the following examples has been written in *C++* with the support of *deal.II* libraries(see [1] for a technical reference). The pictures have been obtained both with Matlab and with IBM Opendx[1].

5.1 Ellipse immersed in a static fluid

The first experiment we present has been developed to examine the influence of the elastic force both on the immersed boundary and on the fluid and to show the good behavior of our model.

The domain Ω is the unit square $]0,1[\times]0,1[$, the immersed boundary initial configuration consists of an ellipse with uniform parametrization

$$\mathbf{X}_0(s) = \begin{pmatrix} 0.2\cos(2\pi s) + 0.3 \\ 0.1\sin(2\pi s) + 0.3 \end{pmatrix} \quad s \in [0,1], \tag{52}$$

approximated by using 618 uniformly spaced nodes.

In Table 1 we report the evolution of the immersed boundary area expressed in percentage with respect to the initial area after 200 time steps. We indicate with m the number of points on the immersed boundary, while N^2 is the number of subsquares of the mesh. We observe that, in order to obtain reasonable results, it seems advisable to have about one segment of the immersed boundary per element.

Figure 2(a) and Figure 2(b) represent respectively the evolution of the boundary during the first 100 time steps and the pressure and fluid velocity at time $t = 1$. As expected the system tends to an equilibrium configuration, which is the circle in a two-dimensional setting.

[1]Deal II and IBM Opendx are Open Source Projects and follow the General Public License. They can be downloaded at *http://www.dealii.org/*, and *http://www.research.ibm.com/dx/*

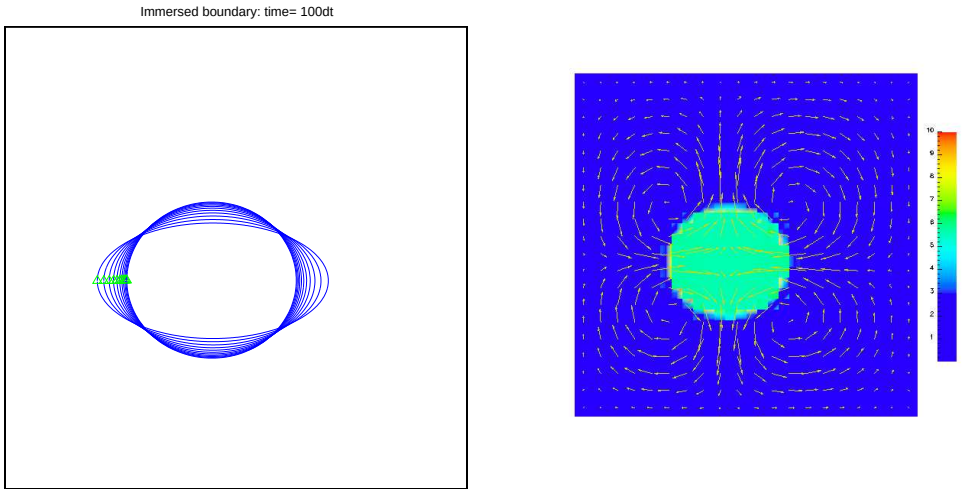

(a) Evolution of the boundary

(b) Fluid pressure and velocity after 100 steps

Figure 2: Evolution of an immersed boundary subjected to its elastic force

5.2 Ellipse immersed in a moving fluid

As an extension to the previous results, we also studied the good behavior of our model when the fluid is driving the motion of the immersed boundary. As we neglet the convective term in the Navier-Stokes equations, we have to add an extra term to the right hand side of (29). More precisely, we add a source term which would give a steady solution $\mathbf{u}_0$, as shown in Figure 3(b). The parameters of this experiments are identical to those of Section 5.1, and the explicit parametrization of the initial configuration $\mathbf{X}_0$ is given in (52).

Figure 3(a) shows how the initial ellipse moves accordingly to the flow and reaches the equilibrium configuration, which is a rotating circle. The rotation is emphasized in the picture by the presence of a green triangle marking a fixed point on the immersed boundary.

5.3 Parametrization dependencies

With the following experiment we want to show the implications of choosing (13) as the tension formulation. We use a non uniform parametrization of the circle centered at the barycenter of Ω, as shown in Figure 4(a).

As expected, the non uniformity of the parametrization reflects the physical meaning of the quantization interval Δs, which is morally a mass. Where the points are farther away from each other, it means that the immersed boundary is more stretched (there is a smaller amount of mass) and tries to reach the equilibrium position shown

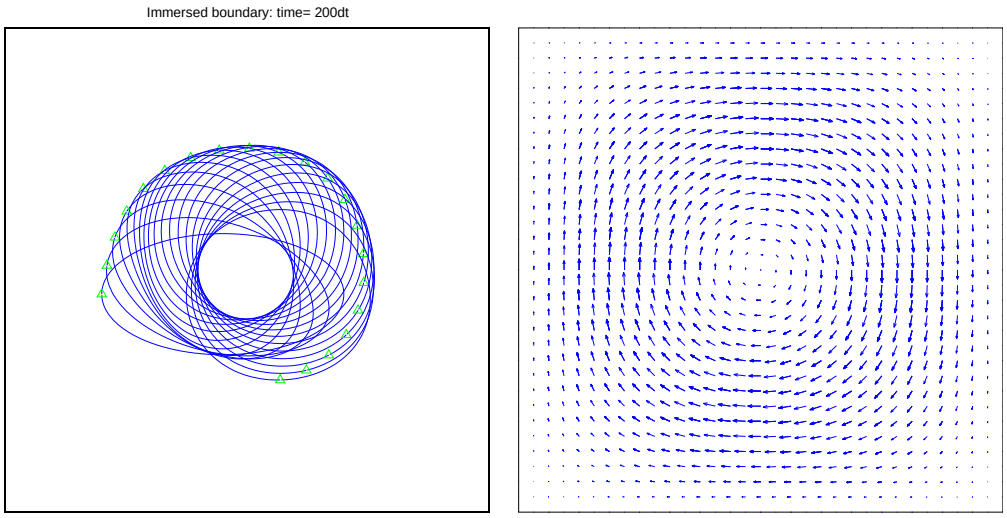

(a) The rotating boundary (b) The rotating fluid

Figure 3: Ellipse driven by a rotating fluid

in Figure 4(c). The actual equilibrium is reached when the resultant of the tangent forces at each point is null, which happens when the ratio between distortion $\Delta \mathbf{X}_i$ and quantization Δs is evenly distributed along the boundary.

5.4 Non closed immersed boundary

Until now we have considered only closed curves immersed in a fluid, neglecting the cases where the boundary is not closed. Let us consider now an elastic string, whose initial configuration is given in Figure 5(a). The behavior of the model follows the tension formulation (51) even if this is not an appropriate description of a physical elastic string. If we do not modify our model, the rest condition for the boundary is when it is collapsed to a single point, which is shown clearly in Figure 5.

This behavior confirms the appropriateness of our model. The incompressibility of the fluid is taken into account in a natural way when the immersed boundary is a closed curve, as pointed out in Example 5.1, but it is also evident when dealing with strings: in Figure 5(c) it is possible to observe how the non-slip condition between the fluid and the string imposes a divergence free motion in the fluid.

5.5 Interaction between immersed boundary and domain boundary

In this test case we show what happens if one or more points of the immersed boundary initial configuration touch the portion of domain boundary $\partial\Omega$ where homoge-

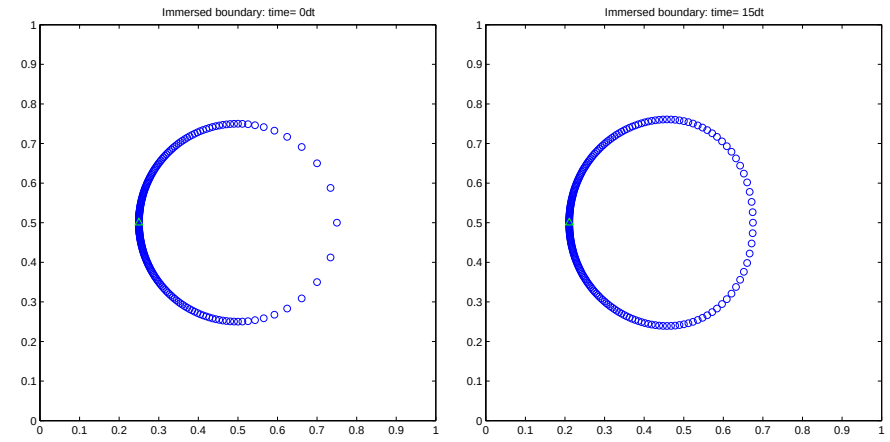

(a) Step 1

(b) Step 15

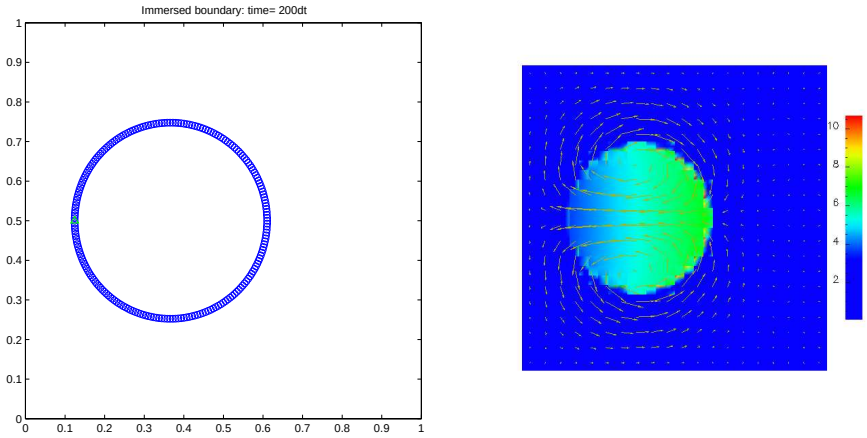

(c) Step 200

(d) Fluid motion and pressure after 100 Steps

Figure 4: Non uniformly parametrized boundary immersed in a static fluid

neous Dirichlet boundary conditions are imposed. We observe that, since the velocity vanishes at those points, then such points of the immersed boundary do not move from their position.

We consider the behavior of a string immersed in a rectangular domain ($\Omega =]0,3[\times]0,1[$) with both ends fixed at $\partial\Omega$, as shown in Figure 6. We use the following source $\mathbf{F}^*(x,y,t)$, which imposes a change of direction to the velocity:

$$\mathbf{F}^*(x,y,t) = \begin{pmatrix} \sin(\pi y)\cos(2\pi t) \\ 0 \end{pmatrix}. \tag{53}$$

As already stated, we impose homogeneous Dirichlet boundary conditions on the hor-

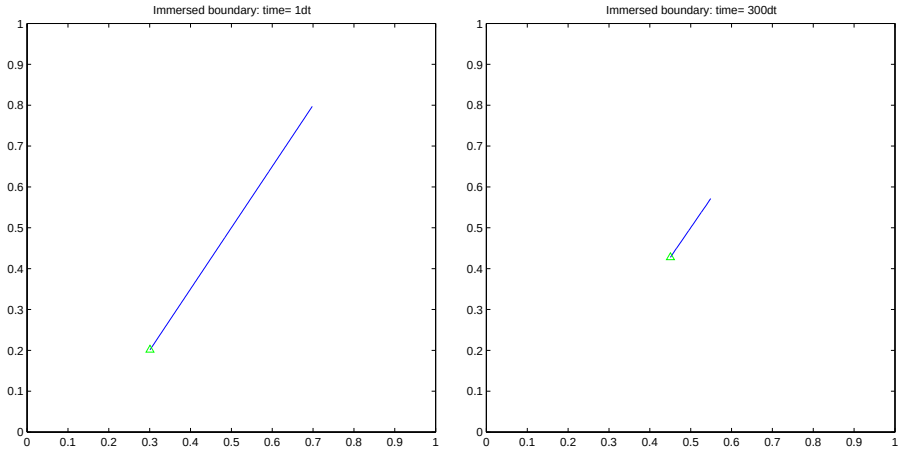

(a) Step 1 (b) Step 300

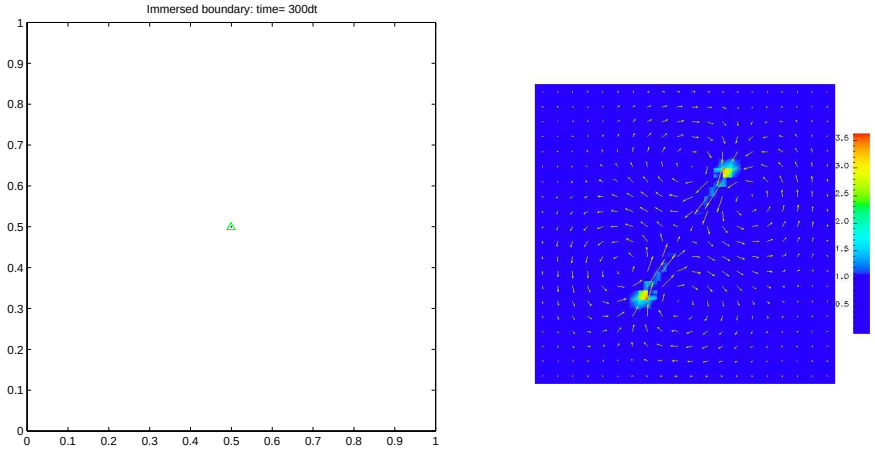

(c) Step 600 (d) The fluid after 100 steps

Figure 5: Non closed elastic string immersed in a static fluid

izontal sides of Ω, while along the vertical sides we have:

$$\mathbf{u}(x,y) = \begin{pmatrix} -\pi^2 \sin(\pi y)\cos(2\pi t) \\ 0 \end{pmatrix} \quad x = 0, 3.$$

5.6 Interaction between two immersed boundaries

This example shows the good behavior of our model when more than one immersed boundary is considered. The domain taken under consideration is the same as in the previous example, with a difference in the load, which generates two laminar flows di-

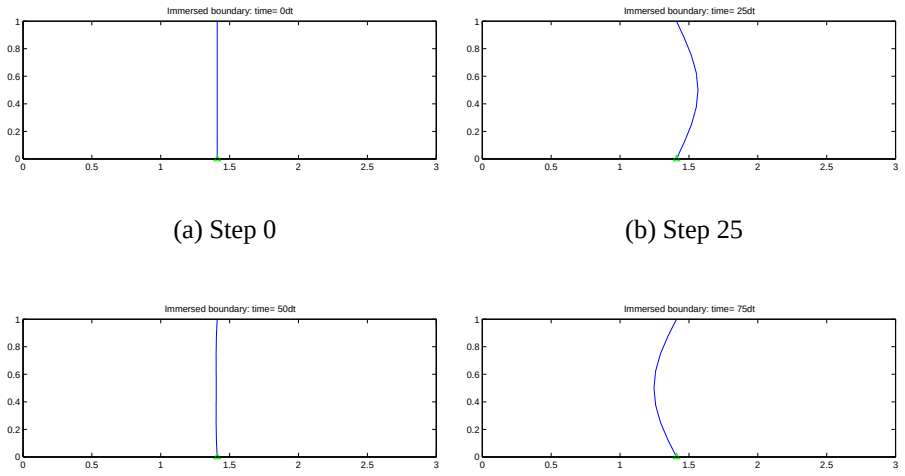

(a) Step 0

(b) Step 25

(c) Step 50

(d) Step 75

Figure 6: Elastic string fixed at the boundary $\partial\Omega$ immersed in a moving fluid

rected in the opposite direction, each of them carrying a different immersed boundary. The expression of the additional source term is given by

$$\mathbf{F}^*(x, y, t) = \begin{pmatrix} \sin(2\pi y) \\ 0 \end{pmatrix}. \tag{54}$$

The initial configuration of the two boundaries was chosen in order to make them as close as possible to each other. Several snapshots of the evolution are reported in Figure 7.

As expected the incompressibility of the fluid influences the behavior of the two immersed boundaries when they approach each other. It is evident that they tend to detach from the horizontal middle axis as soon as they become close enough to feel the presence of the other boundary. It is possible to observe an increase in the pressure of the fluid between the two boundaries, which separates them.

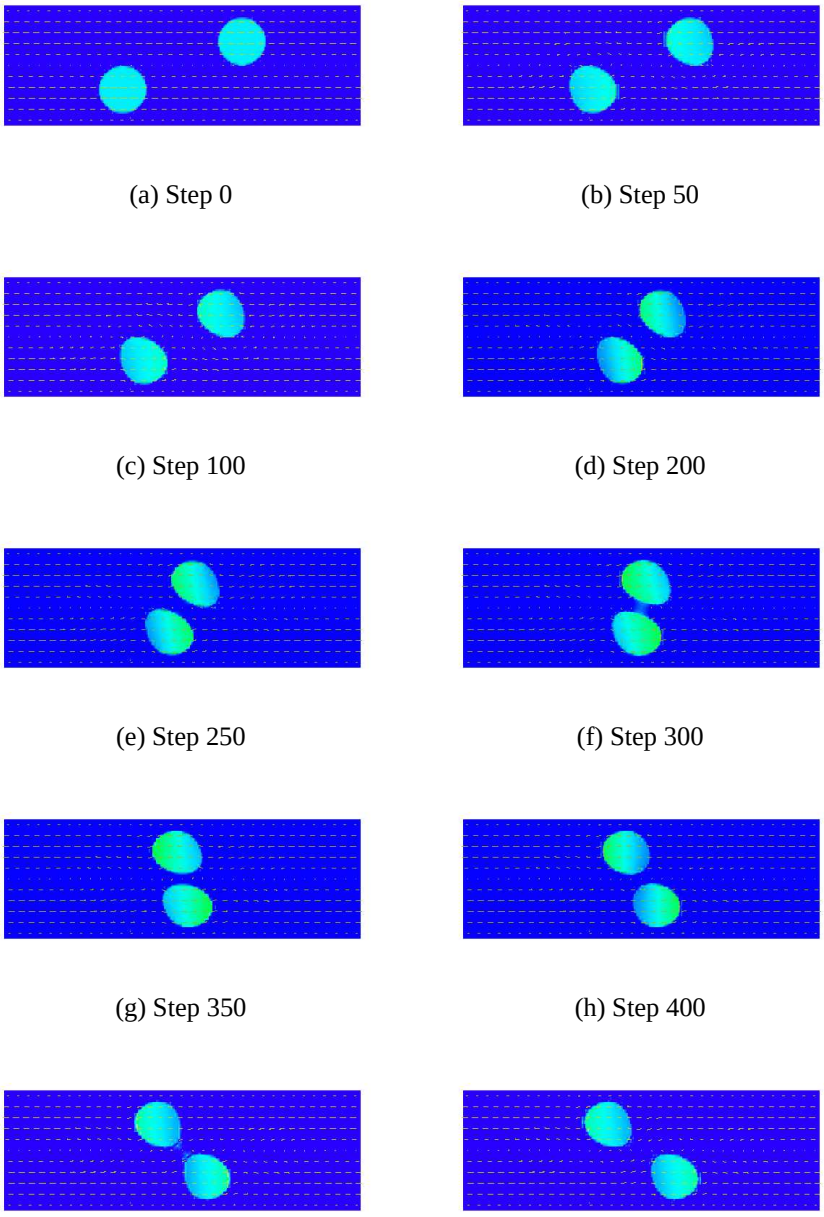

(a) Step 0 (b) Step 50

(c) Step 100 (d) Step 200

(e) Step 250 (f) Step 300

(g) Step 350 (h) Step 400

(i) Step 450 (j) Step 500

Figure 7: Two immersed boundaries driven by laminar flows

6 Finite element discretization of a three dimensional problem

Let us now introduce the finite element discretization of Problem 1 in the case of a three dimensional domain Ω containing a massless membrane.

For simplicity, let us assume that Ω is a polyhedral domain and that there is a massless membrane at rest, fixed at the boundary of Ω; for example, in Fig. 8, the membrane lies along a section of a parallelepiped. Hence, let D be the two dimensional domain

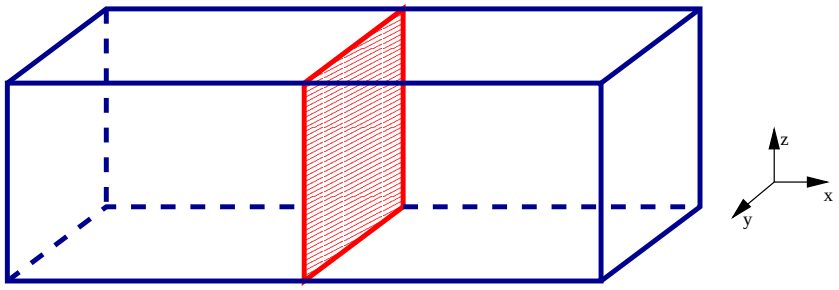

Figure 8: The fluid domain Ω with the immersed boundary (in red) at the initial time.

described by the variable $\mathbf{s} = (r, s)$, which corresponds to the initial configuration of the immersed boundary. In the picture, we have that D occupies a section at some position $x = \bar{x}$ and the variable $\mathbf{s} = (r, s)$ could be the Cartesian variable (y, z). Let us rewrite Problem 1, taking into account the force density defined in (17).

Problem 4 *Given* $\mathbf{f} \in L^2(D \times]0, T[)$, $\mathbf{u}_0 \in H_0^1(\Omega)^3$ *and* $\mathbf{X}_0 : D \to \Omega$, *for all* $t \in]0, T[$, *find* $(\mathbf{u}(t), p(t)) \in H_0^1(\Omega)^3 \times L_0^2(\Omega)$ *and* $\mathbf{X} : D \times]0, T[\to \Omega$, *such that*

$$\rho\left(\frac{d}{dt}(\mathbf{u}(t), \mathbf{v}) + (\mathbf{u} \cdot \boldsymbol{\nabla}\, \mathbf{u}, \mathbf{v})\right) + \mu(\boldsymbol{\nabla}\, \mathbf{u}(t), \boldsymbol{\nabla}\, \mathbf{v})$$
$$- (\nabla \cdot \mathbf{v}, p(t)) =< \mathbf{F}(t), \mathbf{v} > \qquad \forall \mathbf{v} \in H_0^1(\Omega)^3 \qquad (55)$$

$$(\nabla \cdot \mathbf{u}(t), q) = 0 \qquad \forall q \in L_0^2(\Omega) \qquad (56)$$

$$< \mathbf{F}(t), \mathbf{v} >= \int_D \kappa \Delta_{\mathbf{s}} \mathbf{X}(\mathbf{s}, t) \mathbf{v}(\mathbf{X}(\mathbf{s}, t)) \mathrm{d}\mathbf{s} \qquad \forall \mathbf{v} \in H_0^1(\Omega)^3 \qquad (57)$$

$$\frac{\partial \mathbf{X}}{\partial t}(\mathbf{s}, t) = \mathbf{u}(\mathbf{X}(\mathbf{s}, t), t) \qquad \forall \mathbf{s} \in D \qquad (58)$$

$$\mathbf{u}(\mathbf{x}, 0) = \mathbf{u}_0(\mathbf{x}) \qquad \forall \mathbf{x} \in \Omega \qquad (59)$$

$$\mathbf{X}(\mathbf{s}, 0) = \mathbf{X}_0(\mathbf{s}) \qquad \forall \mathbf{s} \in D \qquad (60)$$

$$\mathbf{X}(\mathbf{s}, t) = \mathbf{X}_0(\mathbf{s}) \qquad \forall \mathbf{s} \in \partial D. \qquad (61)$$

We observe that, for $\mathbf{s} \in \partial D$, $\mathbf{X}_0(\mathbf{s})$ are the points of $\partial\Omega$ where the membrane is fixed.

Let $\mathbf{V}_h \subseteq H_0^1(\Omega)^3$ and $Q_h \subseteq L_0^2(\Omega)$ be finite element spaces constructed on a mesh $\mathcal{T}_h$ of Ω made of tetrahedrons or parallelepipeds. We then consider a uniform subdivision $\mathcal{S}_h$ of D into triangles with meshsize h_s and introduce the space of piecewise linear vector valued functions on it:

$$\mathbf{S}_h = \{\mathbf{Y} \in C^0(D;\overline{\Omega}) : \mathbf{Y}_{|K} \in \mathcal{P}^1(K), \forall K \in \mathcal{S}_h, \mathbf{Y}(\mathbf{s}) = \mathbf{X}_0(\mathbf{s})\ \forall \mathbf{s} \in \partial D\}. \quad (62)$$

Let $\mathcal{N}_{hs}$ be the dimension of $\mathbf{S}_h$ (notice that it is equal to the number of internal vertices of $\mathcal{S}_h$). Let $\mathbf{Y} \in \mathbf{S}_h$, then for $i = 1, \ldots, \mathcal{N}_{hs}$, $\mathbf{Y}_i = \mathbf{Y}(\mathbf{s}_i)$ stands for the value of $\mathbf{Y}$ at the node $\mathbf{s}_i$. As in the two dimensional case, when dealing with the discretization of (57), we would like to avoid the computation of $\Delta_{\mathbf{s}}\mathbf{X}_h$ for $\mathbf{X}_h \in \mathbf{S}_h$, hence we use an integration by parts and obtain:

$$< \mathbf{F}(t), \mathbf{v} >= -\kappa \int_D \left(\frac{\partial \mathbf{X}_h(\mathbf{s},t)}{\partial r} \frac{\partial \mathbf{v}(\mathbf{X}_h(\mathbf{s},t))}{\partial r} + \frac{\partial \mathbf{X}_h(\mathbf{s},t)}{\partial s} \frac{\partial \mathbf{v}(\mathbf{X}_h(\mathbf{s},t))}{\partial s} \right) \mathrm{d}\mathbf{s}.$$

We split the integral on the right hand side as the sum over the elements of $\mathcal{S}_h$ and recall that the partial derivatives of $\mathbf{X}_h$ are constant on each element, so that we have for all $\mathbf{v} \in \mathbf{V}_h$:

$$\begin{aligned}
&<\mathbf{F}_h(t), \mathbf{v} > \\
&\quad = -\kappa \sum_{K \in \mathcal{S}_h} \left(\frac{\partial \mathbf{X}_h(t)}{\partial r}\Big|_K \int_K \frac{\partial \mathbf{v}(\mathbf{X}_h(\mathbf{s},t))}{\partial r} \mathrm{d}\mathbf{s} + \frac{\partial \mathbf{X}_h(t)}{\partial s}\Big|_K \int_K \frac{\partial \mathbf{v}(\mathbf{X}_h(\mathbf{s},t))}{\partial s} \mathrm{d}\mathbf{s} \right) \\
&\quad = -\kappa \sum_{K \in \mathcal{S}_h} \left(\frac{\partial \mathbf{X}_h(t)}{\partial r}\Big|_K \int_{\partial K} \mathbf{v}(\mathbf{X}_h(\mathbf{s},t))\, ds - \frac{\partial \mathbf{X}_h(t)}{\partial s}\Big|_K \int_{\partial K} \mathbf{v}(\mathbf{X}_h(\mathbf{s},t))\, dr \right) \\
&\quad = -\kappa \sum_{K \in \mathcal{S}_h} \int_{\partial K} \mathbf{v}(\mathbf{X}_h(\mathbf{s},t)) \left(\frac{\partial \mathbf{X}_h(t)}{\partial r}\, ds - \frac{\partial \mathbf{X}_h(t)}{\partial s}\, dr \right) \\
&\quad = -\kappa \sum_{K \in \mathcal{S}_h} \int_{\partial K} \mathbf{v}(\mathbf{X}_h(t)) \cdot \frac{\partial \mathbf{X}_h(t)}{\partial \mathbf{n}}\, d\sigma
\end{aligned}$$

where $\mathbf{n}$ stands for the outward normal unit vector of ∂K and σ is the curvilinear abscissa along ∂K. We now split the integral along the boundaries of the elements into the sum along each edge, so that taking into account that $\mathbf{v}$ is continuous across the interelement edges and vanishes on ∂D, we obtain

$$< \mathbf{F}_h(t), \mathbf{v} >= -\kappa \sum_{e \in \mathcal{E}_h} \int_e \mathbf{v}(\mathbf{X}_h(t)) \cdot \left[\frac{\partial \mathbf{X}_h(t)}{\partial \mathbf{n}} \right] d\sigma, \quad (63)$$

where $\mathcal{E}_h$ is the set of all internal edges in $\mathcal{S}_h$ and $[\cdot]$ denotes the jump across an edge.

The expression in (63) has the advantage that all the quantities in the integral are well defined, however it should be useful in view of more general applications to write the integral with respect to intrinsic geometric quantities defined along the immersed boundary instead of parametric variables as we have considered here.

Using (63) for the computation of the source term in the discretization of the Navier-Stokes equations, we end up with the following discrete problem:

Problem 5 *Given* $\mathbf{f} \in L^2(D \times]0,T[)$, $\mathbf{u}_{0h} \in \mathbf{V}_h$ *and* $\mathbf{X}_{0h} \in \mathbf{S}_h$, *for all* $t \in]0,T[$, *find* $(\mathbf{u}_h(t), p_h(t)) \in \mathbf{V}_h \times Q_h$ *and* $\mathbf{X}_h(t) \in \mathbf{S}_h$, *such that*

$$\rho\left(\frac{d}{dt}(\mathbf{u}_h(t),\mathbf{v}) + (\mathbf{u}_h \cdot \boldsymbol{\nabla}\,\mathbf{u}_h, \mathbf{v})\right) + \mu(\boldsymbol{\nabla}\,\mathbf{u}_h(t), \boldsymbol{\nabla}\,\mathbf{v})$$
$$- (\nabla\cdot\,\mathbf{v}, p_h(t)) =< \mathbf{F}_h(t), \mathbf{v} > \qquad \forall \mathbf{v} \in \mathbf{V}_h \qquad (64)$$

$$(\nabla\cdot\,\mathbf{u}_h(t), q) = 0 \qquad \forall q \in Q_h \qquad (65)$$

$$< \mathbf{F}_h(t), \mathbf{v} >= -\kappa \sum_{e\in\mathcal{E}_h} \int_e \mathbf{v}(\mathbf{X}_h(t)) \cdot \left[\frac{\partial \mathbf{X}_h(t)}{\partial \mathbf{n}}\right] d\sigma \qquad \forall \mathbf{v} \in \mathbf{V}_h \qquad (66)$$

$$\frac{\partial \mathbf{X}_{h\,i}}{\partial t}(t) = \mathbf{u}_h(\mathbf{X}_{h\,i}(t), t) \qquad \forall i = 1, \cdots, \mathcal{N}_{hs} \qquad (67)$$

$$\mathbf{u}_h(\mathbf{x}, 0) = \mathbf{u}_{0h}(\mathbf{x}) \qquad \forall \mathbf{x} \in \Omega \qquad (68)$$

$$\mathbf{X}_{h\,i}(0) = \mathbf{X}_{0h}(s_i) \qquad \forall i = 1, \cdots, \mathcal{N}_{hs}. \qquad (69)$$

7 Conclusions

We have recalled the formulation of the immersed boundary method and a list of possible application as they can be found in the literature. The key idea is to express the action of the immersed boundary in terms of a concentrated load to the fluid dynamics, governed by the Navier–Stokes equation, by means of a Dirac delta function. Choosing the correct strategy for the approximation of the delta function has been one of the major challenges for the developers of the original immersed boundary method (see, e.g. [27]). In this paper, we presented a finite element approach to the immersed boundary method, according to [4, 5] (for another possible finite element approach, see [36]). The main advantage of our formulation is that we do not need an approximation for the Dirac delta mass, whose action is only seen through its effect onto the test function. We also developed a (mathematically rigorous and physically meaningful) new technique to implement the action of the delta function. This procedure is efficient in terms of computer time and accuracy. Preliminary two dimensional results show the excellent behavior of our approach, where we have used the locally mass preserving Q2/P1 element to approximate the fluid: sharp pressure discontinuities are correctly captured and the scheme does not seem to suffer for any artificial diffusion as it usually happens when the delta function is approximated. Our formulation naturally extends to three space dimensions and to more complex situations; promising 3D numerical results are in progress.

References

[1] W. Bangerth, R. Hartmann, and G. Kanschat, "`deal.II` *differential equations analysis library, technical reference*", `http://www.dealii.org`.

[2] K.J. Bathe, H. Zhang, and S. Ji, *"Finite element analysis of fluid flows fully coupled with structural interactions"*, Computers & Structures, 72, 1-16, 1999.

[3] R.P. Beyer Jr., *"A computational model of cochlea using the immersed boundary method"*, J. Comput. Phys., 98, 145-162, 1992.

[4] D. Boffi and L. Gastaldi, *"A finite element approach for the immersed boundary method"*, Comput. & Structures, 81, 491-501, 2003, In honor of Klaus-Jürgen Bathe.

[5] ———, *"The immersed boundary method: a finite element approach"*, Proc. of the Second M.I.T. Conference on Computational Fluid and Solid Mechanics (K.J. Bathe, ed.), vol. 2, Elsevier, 1263-1266, 2003.

[6] F. Brezzi and M. Fortin, *"Mixed and hybrid finite element methods"*, Springer Series in Computational Mathematics, vol. 15, Springer-Verlag, New York, 1991.

[7] R. Dillon, L. Fauci, A. Fogelson, and D. Gaver III, *"Modeling biofilm processes using the immersed boundary method"*, J. Comput. Phys., 129, 57-73, 1996.

[8] J. Donea, *"Computational methods for transient analysis"*, Computational Methods in Mechanics, vol. 1, ch. Arbitrary Lagrangian Eulerian methods, North-Holland, Elsevier, 1983.

[9] L. J. Fauci and C. S. Peskin, *"A computational model of aquatic animal locomotion"*, J. Comput. Phys., 77, 85-108, 1988.

[10] M. A. Fernández and P. Le Tallec, *"From ALE to transpiration"*, Computational fluid and solid mechanics, Vol. 1, 2 (Cambridge, MA, 2001), Elsevier, Amsterdam, 1166-1169, 2001.

[11] ———, *"Linear stability analysis in fluid-structure interaction with transpiration. I. Formulation and mathematical analysis"*, Comput. Methods Appl. Mech. Engrg., 192, 4805-4835, 2003.

[12] ———, *"Linear stability analysis in fluid-structure interaction with transpiration. II. Numerical analysis and applications"*, Comput. Methods Appl. Mech. Engrg., 192, 4837-4873, 2003.

[13] E. Givelberg, *"Modeling elastic shells immersed in fluid"*, Comm. Pure Appl. Math., 57, 283-309, 2004.

[14] E. Givelberg and J. Bunn, *"A comprehensive three-dimensional model of the cochlea"*, J. Comput. Phys., 191, 377-391, 2003.

[15] R. Glowinski, T. W. Pan, T. I. Hesla, D. D. Joseph, and J. Périaux, *"A fictitious domain approach to the direct numerical simulation of incompressible viscous flow past moving rigid bodies: application to particulate flow"*, J. Comput. Phys., 169, 363-426, 2001.

[16] R. Glowinski, T.-W. Pan, and J. Périaux, *"A fictitious domain method for external incompressible viscous flow modeled by Navier-Stokes equations"*, Comput. Methods Appl. Mech. Engrg., 112, 133-148, 1994, Finite element methods in large-scale computational fluid dynamics (Minneapolis, MN, 1992).

[17] J. G. Heywood and R. Rannacher, *"Finite element approximation of the nonstationary Navier-Stokes problem. I. Regularity of solutions and second-order error estimates for spatial discretization"*, SIAM J. Numer. Anal., 19, 275-311, 1982.

[18] A. Huerta and W. K. Liu, *"Viscous flow with large free surface motion"*, Comput. Methods Appl. Mech. Engrg., 69, 277-324, 1988.

[19] T. J. R. Hughes, W. K. Liu, and T. K. Zimmermann, *"Lagrangian-Eulerian finite element formulation for incompressible viscous flows"*, Comput. Methods Appl. Mech. Engrg., 29, 329-349, 1981.

[20] M.-C. Lai and Z. Li, *"A remark on jump conditions for the three-dimensional Navier-Stokes equations involving an immersed moving membrane"*, Appl. Math. Lett., 14, 149-154, 2001.

[21] M.-C. Lai and C. S. Peskin, *"An immersed boundary method with formal second-order accuracy and reduced numerical viscosity"*, J. Comput. Phys., 160, 705-719, 2000.

[22] P. L. Le Tallec and J. Mouro, *"Fluid structure interaction with large structural displacements"*, Comput. Methods Appl. Mech. Engrg., 190, 3039-3067, 2001.

[23] M. Lesoinne and C. Farhat, *"Geometric conservation laws for flow problems with moving boundaries and deformable meshes and their impact on aeroelastic computations"*, Comput. Methods Appl. Mech. Engrg., 134, 71-90, 1996.

[24] W. K. Liu, S. Jun, and Y. F. Zhang, *"Reproducing kernel particle methods*, Internat. J. Numer. Methods Fluids, 20, 1081-1106, 1995, Finite elements in fluids—new trends and applications (Barcelona, 1993).

[25] D. M. McQueen and C. S. Peskin, *"Heart simulation by an immersed boundary method with formal second-order accuracy and reduced numerical viscosity"*, Mechanics for a New Millennium, Proceedings of the International Conference on Theoretical and Applied Mechanics (ICTAM) 2000 (H. Aref and J. W. Phillips, eds.), Kluwer Academic Publishers, 2001.

[26] T. Nomura and T. J. R. Hughes, *"An arbitrary Lagrangian-Eulerian finite element method for interaction of fluid and rigid body"*, Comput. Methods Appl. Mech. Engrg., 95, 115-138, 1992.

[27] C. S. Peskin, *"The immersed boundary method"*, Acta Numerica, 2002, Cambridge University Press, 2002.

[28] C. S. Peskin and D. M. McQueen, *"A three-dimensional computational method for blood flow in the heart. I. Immersed elastic fibers in a viscous incompressible fluid"*, J. Comput. Phys., 81, 372-405, 1989.

[29] ———, *"Computational biofluid dynamics"*, Fluid dynamics in biology (Seattle, WA, 1991), Contemp. Math., vol. 141, Amer. Math. Soc., Providence, RI, 1993, pp. 161-186.

[30] C. S. Peskin and B. F. Printz, *"Improved volume conservation in the computation of flows with immersed elastic boundaries"*, J. Comput. Phys., 105, 33-46, 1993.

[31] C.S. Peskin, *"Numerical analysis of blood flow in the heart"*, J. Computational Phys., 25, 220-252, 1977.

[32] A. Quarteroni, *"Modeling the cardiovascular system: a mathematical challenge"*, Mathematics Unlimited – 2001 and Beyond, (B. Engquist and W. Schmid, eds.), Springer-Verlag, 2001, pp. 961-972.

[33] P. Raj and B. Harris, *"Using surface transpiration with an euler method for cost-effective aerodynamic analysis"*, AIAA 24th Applied Aerodynamics Conference

(Monterey, Canada), 1993.

[34] M. E. Rosar and C. S. Peskin, *"Fluid flow in collapsible elastic tubes: a three-dimensional numerical model"*, New York J. Math., 7, 281-302, 2001 (electronic).

[35] X. Wang and W.K. Liu, *"Extended immersed boundary method using FEM and RKPM"*, Comput. Methods Appl. Mech. Engrg., 193, 1305-1321, 2004.

[36] L. Zhang, A. Gerstenberger, X. Wang, and W.K. Liu, *"Immersed finite element method"*, Comput. Methods Appl. Mech. Engrg., 193, 2051-2067, 2004.

[37] L. Zhu and C. S. Peskin, *"Simulation of a flapping flexible filament in a flowing soap film by the immersed boundary method"*, J. Comput. Phys., 179, 452-468, 2002.

[38] ———, *"Interaction of two flapping filaments in a flowing soap film"*, Phys. Fluids, 15, 1954-1960, 2003.